CIVIL AND ENVIRONMENTAL ENGINEERING REPORTS

E-ISSN 2450-8594

CEER 2026; 36 (2): 0016-0036
DOI: 10.59440/ceer/221723
Original Research Article

INFLUENCE OF FILLER CONTENT AND POLYMER COMPOSITION ON THE PROPERTIES, MORPHOLOGY AND PROCESSING PARAMETERS OF BIODEGRADABLE COMPOSITES

Joanna TOMASIK[1], Tomasz GARBACZ[2], Aneta TOR-ŚWIĄTEK[2]
[1] Department of Technology and Polymer Processing, Lublin University of Technology, Lublin University of Technology Doctoral School, Lublin, Poland
[2] Department of Technology and Polymer Processing, Lublin University of Technology, Lublin, Poland

A b s t r a c t

Biodegradable composites based on PLA, PHB and a PLA/PHB (80:20) blend with 0, 5 and 10 wt% wood fibers were injection molded into ISO 527 Type 1A specimens. Samples were produced on an Engel Victory 200/50 fast track injection molding machine using a two channel, uncooled mold. Density, Shore D hardness, tensile properties, unnotched impact strength and fracture surfaces were examined. Wood fibers caused small increases in density and only minor changes in hardness, but consistently raised Young's modulus. At the same time, they reduced tensile strength, elongation at break and impact strength, leading to material embrittlement. The polymer matrix determined the baseline stiffness and ductility, while fiber content shifted the stiffness-toughness balance and increased variability at 10 wt% filler. Microscopy confirmed brittle fracture with fibers dispersed throughout the matrices.

Keywords: biodegradable polymer composites, polylactic acid (PLA), poly(3-hydroxybutyrate) (PHB), wood fibers, injection molding

1. INTRODUCTION

Plastic materials are extensively utilized across modern industrial sectors and everyday applications. They are commonly employed in packaging, construction, automotive components, electronics and medical devices. Published research highlights that plastics have profoundly transformed the automotive industry, enabling advanced vehicle design, substantial weight reduction, enhanced safety performance and progress toward more sustainable manufacturing [1]. Plastics have also become indispensable in medicine, where synthetic and biodegradable polymers are widely used in e.g. medical devices, wound dressings and implants [2, 3]. The extensive use of plastics is driven by their favorable properties,

[1] Corresponding author: Department of Technology and Polymer Processing, Lublin University of Technology, Lublin University of Technology Doctoral School, Nadbystrzycka 36, 20-618 Lublin, s101049@pollub.edu.pl, + 48 81 538-42-21

affordability and adaptability, resulting in a rapid rise in global consumption in recent decades. The majority of plastics are not biodegradable and can remain in the environment for centuries. Only a minor portion of plastic waste is recycled, while most is deposited in landfills, incinerated, or left uncollected [4]. Only about 25% of end of life macroplastic waste is currently recovered through mechanical recycling, while the majority remains unrecycled. The use of chemical recycling to convert plastics into chemicals, fuels, lubricants, or paraffin waxes is still being explored [5].

The most popular biodegradable materials are polylactic acid (PLA) and poly(3-hydroxybutyrate) (PHB). PLA is a biobased polyester derived from lactic acid typically obtained by fermentation of renewable biomass and PHB is a microbial polyester produced by bacteria [6, 7]. Thanks to their biodegradability or compostability under appropriate conditions, they can serve as a more environmentally friendly alternative to petroleum based plastics [6]. Both PLA and PHB exhibit relatively high brittleness, low impact resistance and limited elongation at break, which restricts their use in applications requiring significant deformation or high impact strength [8]. Moreover, PHB is often criticized for processing difficulties due to its narrow melting temperature range and tendency for thermal degradation, which limits its manufacturability [9]. PLA is a relatively brittle material with limited impact resistance, which represents a significant limitation for many applications [8]. Therefore, current research is focused on PLA/PHB blends, composites reinforced with natural fibers or nanoparticles and plasticizer modifications, aiming to achieve a balance between biodegradability and mechanical as well as processing properties [10].

Natural fillers such as wood flour [11], flax fibers [12], hemp fibers [13] and corn fibers [14] are widely used in polymer composites to modify specific properties while reducing environmental impact. These organic fillers are typically renewable, biodegradable and often inexpensive or derived from waste, making them an alternative to synthetic reinforcements [11- 14]. Incorporating organic fillers often decreases tensile strength and impact resistance due to stress concentration around filler particles and imperfect interfacial bonding. Issues such as poor dispersion within the polymer matrix and increased brittleness can further restrict performance in demanding applications [8]. The filler content and type play a crucial role in determining the final properties of the composite. Similarly, the choice of filler size, aspect ratio and surface chemistry significantly affects mechanical performance, processability and the balance between stiffness and toughness [15].

Comprehensive research is necessary to examine not only the physical and mechanical properties of these composites but also their processing parameters. Such integrated studies provide crucial insights into how variations in filler type, content, and dispersion affect the final properties and processability of the material. This knowledge is particularly important in the design of packaging materials, structural components, and other environmentally friendly products, where both performance and sustainability are key considerations [16].

The present study aims to evaluate the influence of wood fiber mass fraction and polymer matrix type on the physical, mechanical, and processing properties of biodegradable composites. By systematically investigating PLA, PHB, and PLA/PHB blends with varying filler content, this research also addresses the selection of processing parameters for these materials. The findings are expected to support the development of new composites that combine environmental sustainability with practical mechanical and processing properties, enabling broader adoption in industrial applications.

2. MATERIALS AND METHODS

The materials used in this study were polylactic acid - PLA (Ingeo 3251D, distributed by RESINEX, produced by NatureWorks LLC, USA), poly(3-hydroxybutyrate) - PHB (Biomer P304, Biomer, Germany) and their blend at a mass ratio of 80:20 (PLA:PHB).

The PLA grade (Ingeo 3251D) is characterized by a density of 1240 kg/m^3. Its tensile strength reaches 62.1 MPa, while the elongation at break remains at 3.5%. The notched Izod impact strength was determined to be 16 J/m.

The PHB grade (Biomer P304) is characterized by a density of 1250 kg/m^3 and a Shore D hardness of 67 ShD. The material exhibits a Young's modulus in the range of 1140-1900 MPa and a tensile strength of 24-27 MPa, with an elongation at break of 6-9%. PHB also demonstrates relatively high impact resistance in the unnotched configuration, with an impact strength of 82.9 kJ/m^2.

For each polymer matrix, a set of three material variants was prepared: neat polymer (without filler) and composites containing 5 wt% and 10 wt% wood fibers. The wood fibers used as filler were ARBOCEL C 320 (J. RETTENMAIER & SÖHNE GmbH + Co KG, Germany), a natural cellulose material obtained from renewable raw sources. The fibers have a beige, cubic morphology with an average particle size in the range of 200-500 μm and a bulk density of 160-240 g/dm^3. According to sieve analysis 80% of the particles pass through a 100 μm mesh. The appearance of the polymer granules, the wood filler, and the composite is presented in Figure 1.

The components of each composition were weighed using a Radwag WPE2000 (Radwag, Poland) analytical balance with an accuracy of 0.1 g and then manually mixed in plastic containers to ensure homogeneity. The measured moisture content of the raw materials was 0.37% for PLA, 0.8% for PHB and 2.76% for wood fibers. The prepared specimens were molded into standardized dumbbell shapes for mechanical testing and are shown in Figure 2.

Fig. 1. Materials used for sample preparation: from left: PLA granules, PHB granules, wood fibers and a PLA/PHB (80:20) blend containing 10 wt% wood fibers

Fig. 2. Photographs of the prepared dumbbell specimens under natural light, categorized by matrix material and filler content. From left to right: PLA, PHB and PLA/PHB (80:20) blend. Within each group, the samples represent 0 wt%, 5 wt% and 10 wt% wood fiber content, respectively

For the fabrication of the test specimens, a tie-bar-less Engel Victory 200/50 fast track servohydraulic injection molding machine (Engel Austria GmbH, Austria) was used (Figure 3a). The machine is equipped with a clamping force of 500 kN and a modular injection unit with a 30 mm screw. The samples were produced using a two channel, noncooled mold (Figure 3b). The mold cavity consisted of two Type 1A paddle shaped cavities. Specimens as defined in PN-EN ISO 527-2 [17]. For type 1A the standard dimensions are: total length 170 mm, length of parallel section 80 mm, gauge section width 10 mm, thickness 4 mm.

a) b)

Fig. 3. Injection molding machine used for the fabrication of test specimens: a) general view of the Engel Victory 200/50 Fast Track injection molding machine, b) close-up of the two channel mold with Type 1A specimen cavities

The selected injection molding parameters for the materials: PHB, PLA and the PLA/PHB (80:20) blend are presented in Table 1. The injection process was carried out using material specific injection pressures of 400 bar for PHB, 700 bar for PLA and 500 bar for the PLA/PHB blend, with a constant shot volume of 36 cm^3, while the temperature and holding pressure profiles were established based on material datasheets and subsequently refined through experimental optimization. For the PLA/PHB (80:20) system, a compromise temperature profile was required to ensure adequate melting of both components while preventing thermal degradation of the material with the lower thermal stability.

For PHB the temperature settings were referenced from the manufacturer's recommendations for the cylinder zones: 145/155/165/180°C. However, in the present study the applied four zone temperature profile was adjusted to 165/180/165/150°C. This increase in processing temperature was introduced to facilitate the subsequent blending of PHB with PLA and to maintain, as far as possible, comparable processing conditions across all three matrix types. For PLA, the material datasheet indicates significantly higher injection molding temperatures: rear zone from 166 to 177°C, middle zone from 182 to 193°C, front zone from 188 to 204°C and nozzle from 188 to 204°C. In the experiments reported here, a reduced cylinder profile of 160/170/165/155°C was applied for PLA and the same profile was used for the PLA/PHB (80:20) blend. This deliberately flattened and lowered temperature profile, relative to the recommendations for neat PLA, was selected to limit thermal degradation of the more temperature sensitive PHB while still ensuring sufficient melting of both components within the blend.

The time and pressure parameters for injection molding were established individually for each material due to inherent differences in their flow behavior, melt viscosity and thermal characteristics. The injection time was set to 0.99 s for PHB, 1.21 s for PLA and 0.87 s for the PLA/PHB (80:20) blend. These values were adjusted to account for the distinct viscosity profiles and solidification rates of the polymers, ensuring complete cavity filling under stable flow conditions and preventing defects such as short shots. The short shots observed in PLA and in the PHB specimens are presented in Figure 4a, whereas the surface irregularities and defects in PLA sample are shown in Figure 4b.

A three stage holding pressure profile was applied, with corresponding pressure levels of 100/200/300 bar for PHB, 600/750/900 bar for PLA and 300/500/750 bar for PLA/PHB (80:20) blend. The holding times: 15 s for PHB, 7 s for PLA and 13 s for the PLA/PHB (80:20) blend were selected to compensate for the different shrinkage behaviors, melt compressibility and pressure build characteristics of the materials.

Cooling times were set to 30 s, 35 s and 25 s for PHB, PLA and PLA/PHB, respectively. The mold temperature was maintained at 30 °C for PHB and PLA and at 24 °C for the PLA/PHB blend. These adjustments ensured proper mold filling, minimized internal stresses and enabled the production of dimensionally stable samples of satisfactory surface quality across all material systems.

During parameter optimization, the holding phase proved critical for achieving the required surface quality. Due to the presence of surface waviness in the molded parts indicative of insufficient packing and incomplete shrinkage compensation, the holding pressure was incrementally increased in steps of 100 bar until specimens with satisfactory surface characteristics were obtained. Adjusting the holding pressure profile served as the primary means of improving surface appearance and dimensional stability across all material systems.

Table 1. Selected injection molding parameters for the three materials: PHB, PLA and PLA/PHB (80:20)

Parameter	**Unit**	**PHB matrix**	**PLA matrix**	**PLA/PHB (80:20) matrix**
Temperature profile	°C	165, 180, 165, 150	160, 170, 165, 155	160, 170, 165, 155
Injection pressure	bar	400	700	500
Shot volume	cm^3	36	36	36
Injection time	s	0.99	1.21	0.87
Holding pressure profile	bar	100, 200, 300 (15/7.5/0 s)	600, 750, 900 (7/3.5/0 s)	300, 500, 750 (13/6.5/0 s)
Holding time	s	15	7	13
Cooling time	s	30	35	25
Mold temperature	°C	30	30	24
Total cycle time	s	56.93	54.15	49.81

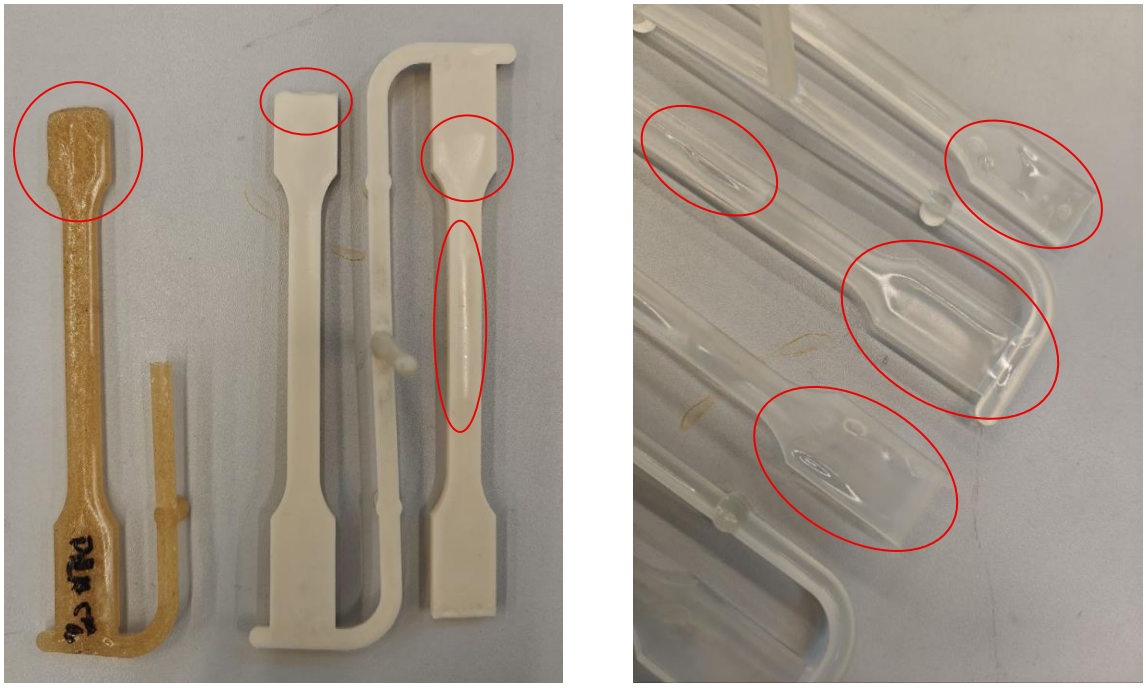

a) b)

Fig. 4. Examples of defects observed in the early stages of injection molding: a) incomplete specimens with missing end sections of the paddles: on the left, PLA containing 5 wt% wood fibers (only one side is present because the connecting runners between specimens occasionally broke during ejection from the machine) and on the right, a specimen produced from neat PHB, b) a specimen made of neat PLA, showing an uneven, wavy surface resulting from inadequate injection parameters

The moisture content was determined using a Radwag WPS 50 SX (Radwag, Poland) moisture analyzer based on the thermogravimetric method, at a drying temperature of 90°C, with the measurement terminated when the mass change was below 1 mg per 120 s.

The density measurements were carried out using a Radwag AS 82/220.R2 (Radwag, Poland) analytical balance equipped with a density determination kit for solids and liquids. The measurements were performed using isopropanol as the immersion medium. The balance has a maximum capacity of 220 g, a readability of 0.1 mg.

The Shore hardness measurements were performed using an AFFRI ART.13 hardness tester (AFFRI, Italy) in accordance with PN-EN ISO 868 [18], using the Shore D scale.

The tensile tests were performed using a Shimadzu EZ-Test-LX (Shimadzu Corporation, Japan) universal testing machine with a single column frame. The system was equipped with a 5 kN load cell and allowed a testing speed range from 0.001 to 2000 mm/min. Data acquisition and control were managed using TRAPEZIUM X software. The specimens were standardized dumbbell shaped specimens prepared in accordance with PN-EN ISO 5270-1 [19] and tested at a speed of 50 mm/min. Figure 5 presents the specimens after tensile testing for all material types.

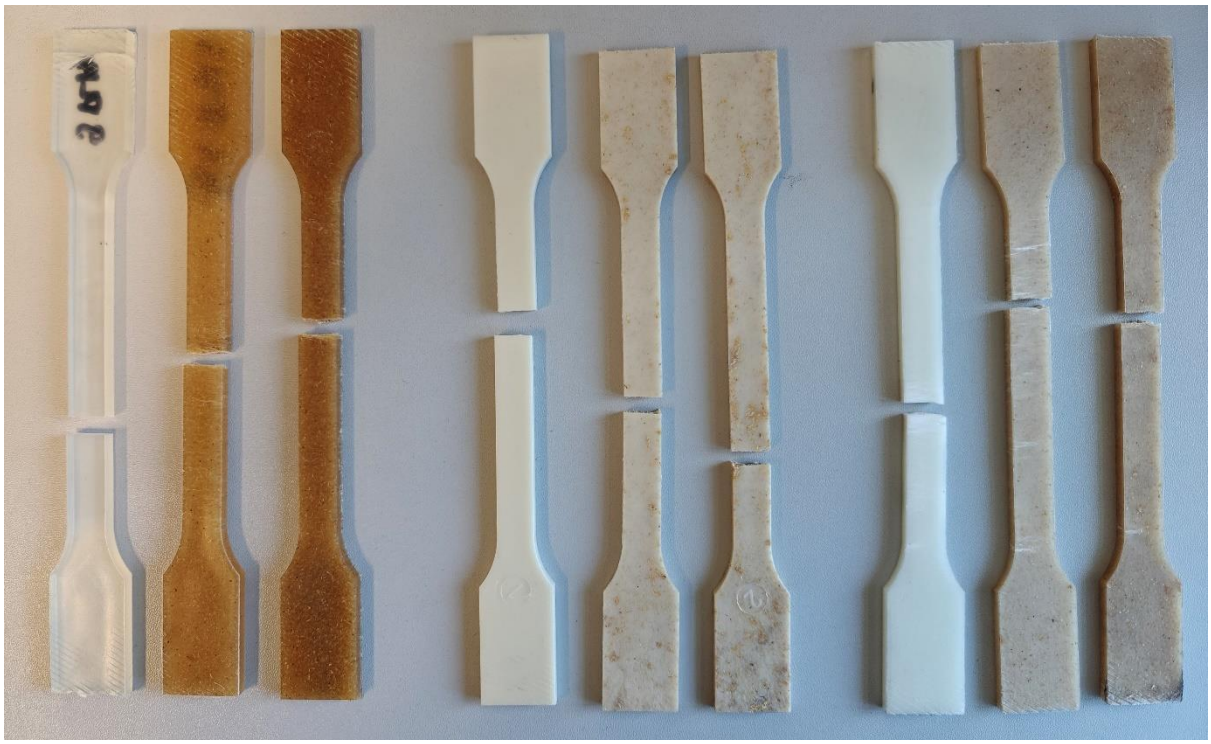

Fig. 5. Specimens after tensile testing. From left to right, the groups correspond to samples with PLA, PHB and PLA/PHB (80:20) matrices. Within each group, the samples contain 0, 5 and 10 wt% of wood fibers, respectively

The impact tensile tests were carried out using a QC-6939J-3 apparatus (Cometech Testing Machines Co., Ltd., Taiwan). The test specimens were standardized rectangular bars, with approximate dimensions of 80 mm x 10 mm x 4 mm, prepared in accordance with PN-EN ISO 8256 [20], Method A, without notches. A 2 J pendulum hammer and a transverse grip were used during testing.

The structural analysis was performed using a Nikon Eclipse LV100ND (Nikon Corporation, Japan) microscope. Observations were conducted at magnifications of 2.5X, 5X and 10X under various imaging conditions, including bright field, dark field, polarized light and differential interference contrast. Observations were primarily carried out using transmitted light.

3. RESULTS

Figure 6 shows the results of density measurements, while Figure 7 illustrates the Shore D hardness values for all tested materials. The subsequent graphs (Figures 8-10) depict the results of the tensile tests, including tensile strength, elongation at break and Young's modulus, respectively. Figure 11 presents the results of the impact strength measurements. Additionally, Figures 12-20 show the microscopic images of the fracture surfaces of the specimens after failure as well as the surface morphology, obtained using an optical microscope.

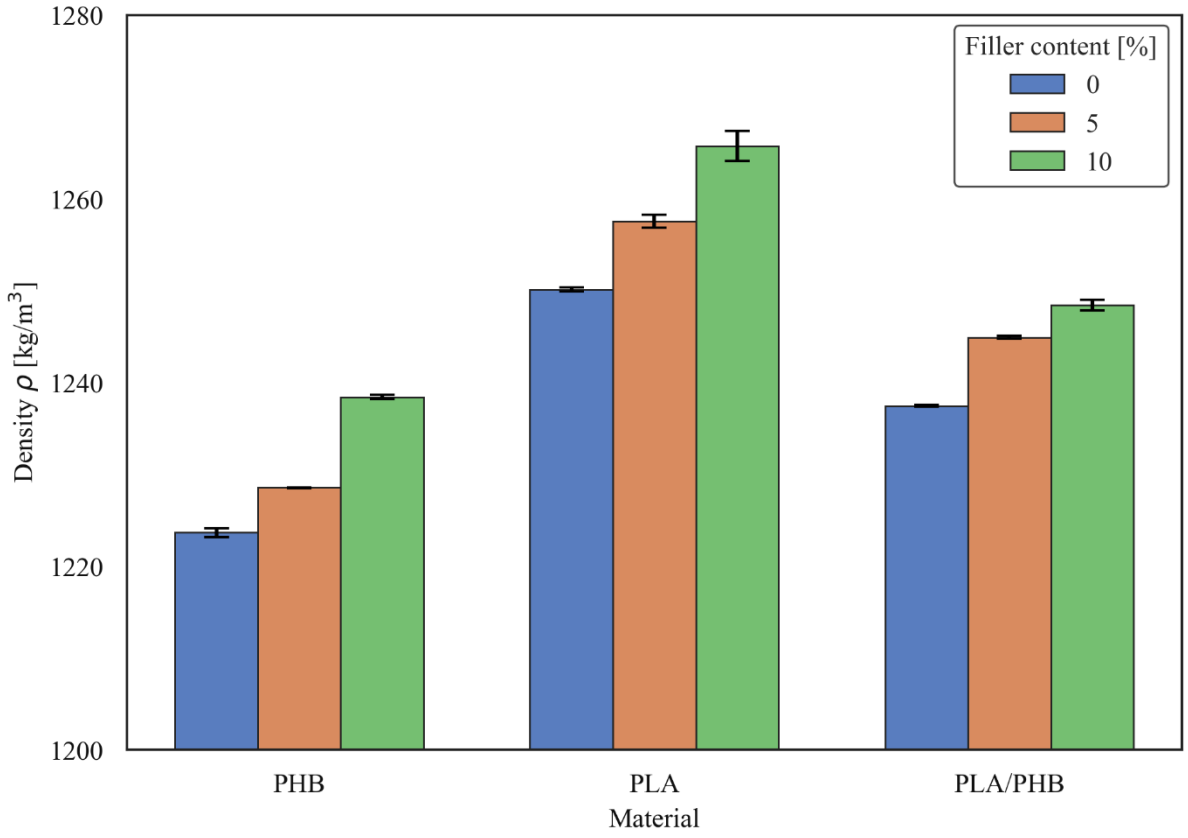

Fig. 6. Density of PLA, PHB and PLA/PHB (80:20) composites containing different amounts of wood fibers (0, 5 and 10 wt%)

Figure 6 presents the density values of PHB, PLA, and PLA/PHB (80:20) composites containing 0, 5, and 10 wt% wood fiber filler. For PHB, the neat polymer exhibited a density of 1223.6 kg/m^3, which is slightly lower than the reference value for Biomer P304 (1250 kg/m^3). A slight increase in density was observed with increasing filler content, reaching the highest values at 10 wt%,

corresponding to an overall increase of about 1.2%. PLA showed an initial density of 1250.1 kg/m^3, closely matching the datasheet value for Ingeo 3251D (1240 kg/m^3). With filler addition, the density increased gradually, corresponding to an increase of around 1.3% relative to the neat polymer. The PLA/PHB (80:20) blend exhibited intermediate density values between the neat polymers, with a slight increase of approximately 0.9% upon filler addition. A minor increase in standard deviation was observed at higher filler loading, particularly for PLA at 10 wt%, indicating slightly reduced homogeneity of filler distribution. Overall, the results suggest that the polymer matrix largely determines the density, while wood fiber addition up to 10 wt% leads to only modest, systematic increases.

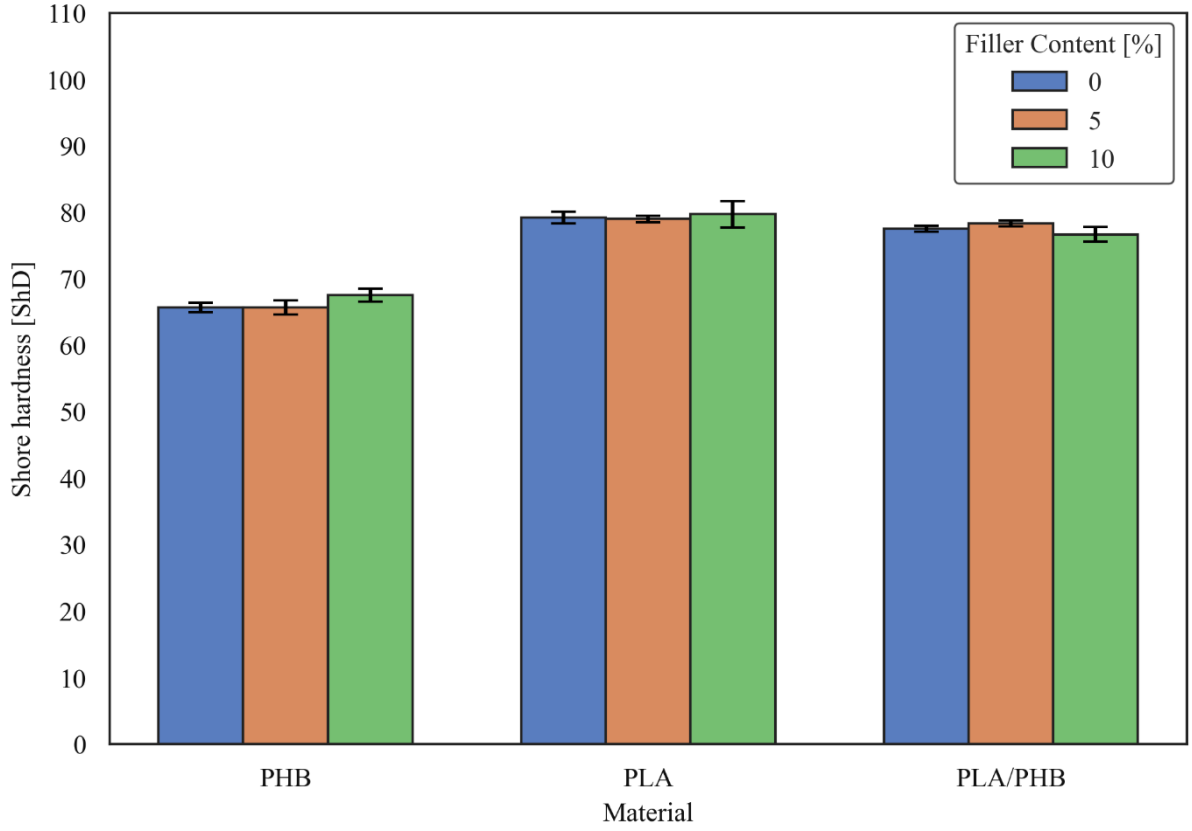

Fig. 7. Shore D hardness of PLA, PHB and PLA/PHB (80:20) composites containing different amounts of wood fibers (0, 5 and 10 wt%)

Figure 7 presents the Shore D hardness values of PHB, PLA, and PLA/PHB composites containing 0, 5, and 10 wt% filler. Overall, PLA exhibited the highest hardness (around 79 ShD), with minimal variation across filler contents, indicating that the matrix governs the mechanical response and that filler addition up to 10 wt% has no significant effect. PHB exhibited lower hardness, with the neat material at 65.7 ShD (close to the datasheet value of 67 ShD) and a slight increase to 67.5 ShD at 10 wt%, corresponding to a marginal improvement of approximately 2.8%. The PLA/PHB blend exhibited intermediate hardness values, approximately 2-3% lower than neat PLA, reflecting the softening effect of the PHB phase. Filler addition caused only minor variations across all materials, with a slight increase at 5 wt% and a small decrease at 10 wt%. A general increase in standard deviation with higher filler content, particularly at 10 wt%, suggests reduced filler dispersion uniformity and local microstructural

heterogeneity. Overall, the results indicate that hardness is primarily governed by the polymer matrix type, while wood fiber addition up to 10 wt% has only minor or statistically insignificant effects.

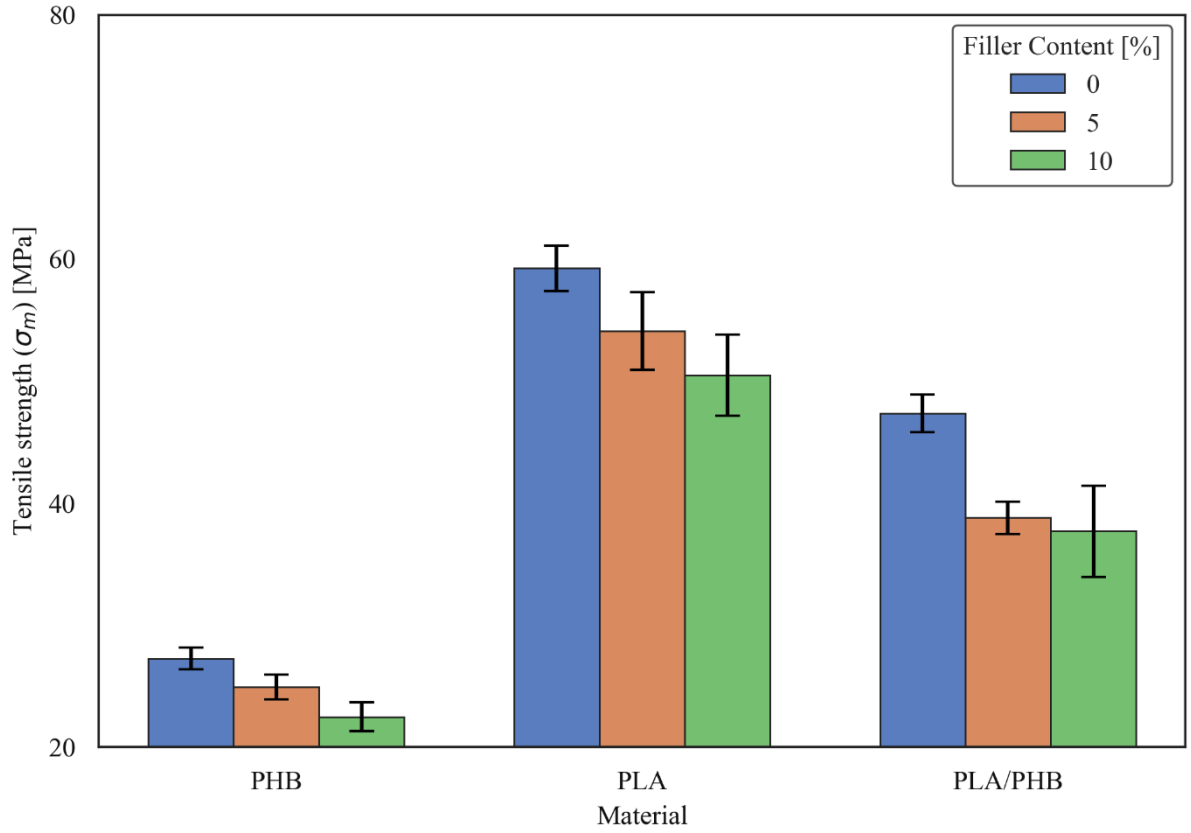

Fig. 8. Tensile strength of PLA, PHB and PLA/PHB (80:20) composites containing different amounts of wood fibers (0, 5 and 10 wt%)

The tensile strength results revealed clear differences between the tested materials and a consistent reduction with increasing wood fiber content. Among the neat polymers, PLA exhibited the highest tensile strength (59.23 MPa), followed by the PLA/PHB (80:20) blend and PHB, reflecting the intrinsic differences between the matrices. In all cases, wood fiber addition led to a reduction in tensile strength. The PLA/PHB (80:20) blend showed intermediate performance compared to the neat polymers. According to the literature, the tensile strength of PLA/PHB (75:25) is 45.1 MPa, which is consistent with the value obtained in this study [17]. Overall, the observed reduction in tensile strength with increasing filler content is attributed to stress concentration at the fiber-matrix interface and limited interfacial adhesion, which promotes premature failure under load. This reflects the combined effect of the softer PHB phase and the presence of the wood fiber filler, where the PHB component reduces the overall load-bearing capacity of the blend due to its lower intrinsic strength and stiffness compared to PLA, while the dispersed wood fibers act as stress concentration sites that promote interfacial debonding and early crack initiation under tensile loading.

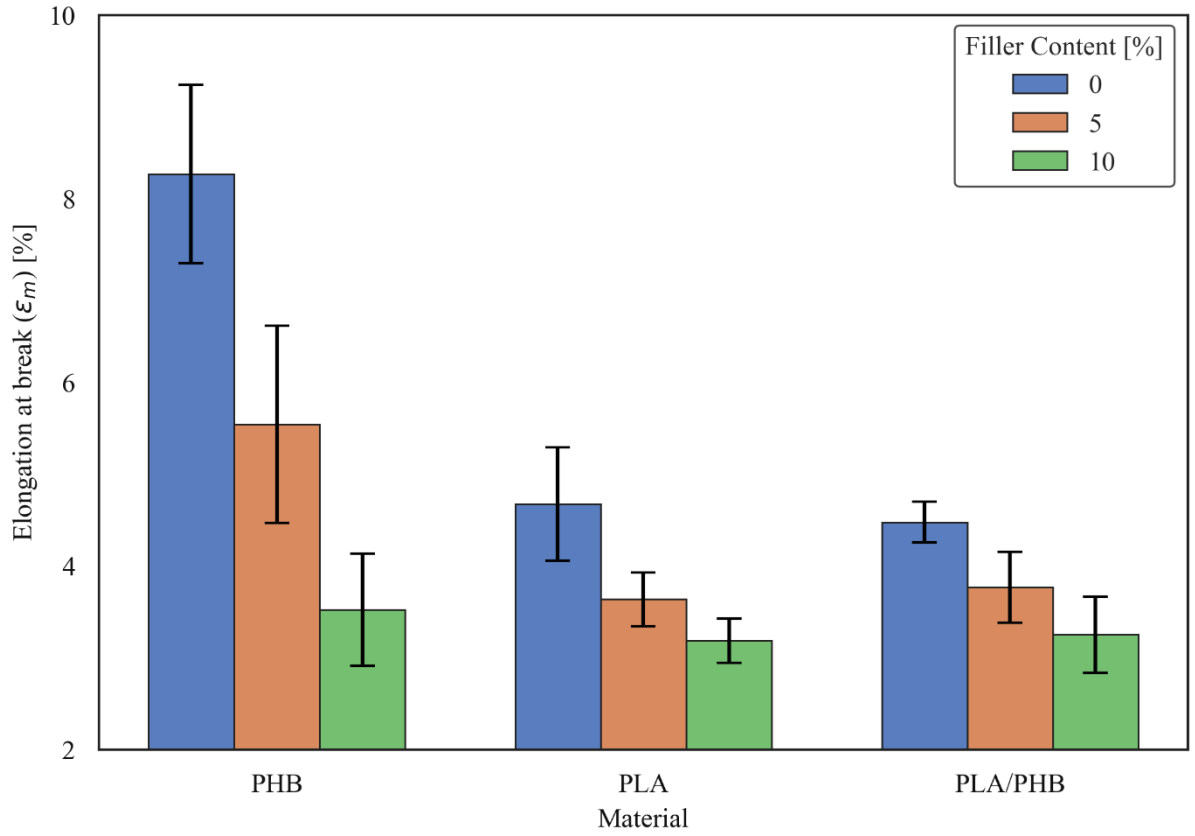

Fig. 9. Elongation at break of PLA, PHB and PLA/PHB (80:20) composites containing different amounts of wood fibers (0, 5 and 10 wt%)

The elongation at break values showed a clear decreasing trend with increasing wood fiber content for all tested materials. Among the neat polymers, PHB exhibited the highest ductility (8.27%), followed by PLA and the PLA/PHB (80:20) blend, reflecting differences in chain mobility and matrix structure. In all systems, wood fiber addition led to a progressive reduction in elongation at break, indicating a loss of deformability and increased brittleness. The most pronounced decrease was observed for PHB, where elongation dropped to 3.52% at 10 wt% filler. Similar reductions were observed for PLA and the PLA/PHB blend, confirming a consistent embrittlement effect across all materials. The PLA/PHB (80:20) blend showed intermediate ductility compared to the neat polymers. According to the literature, the elongation at break of PLA/PHB (75:25) is 4.6%, which is consistent with the value obtained in this study [17]. Overall, the reduction in elongation at break is attributed to restricted polymer chain mobility caused by the presence of wood fibers, which increases stiffness and reduces material deformability.

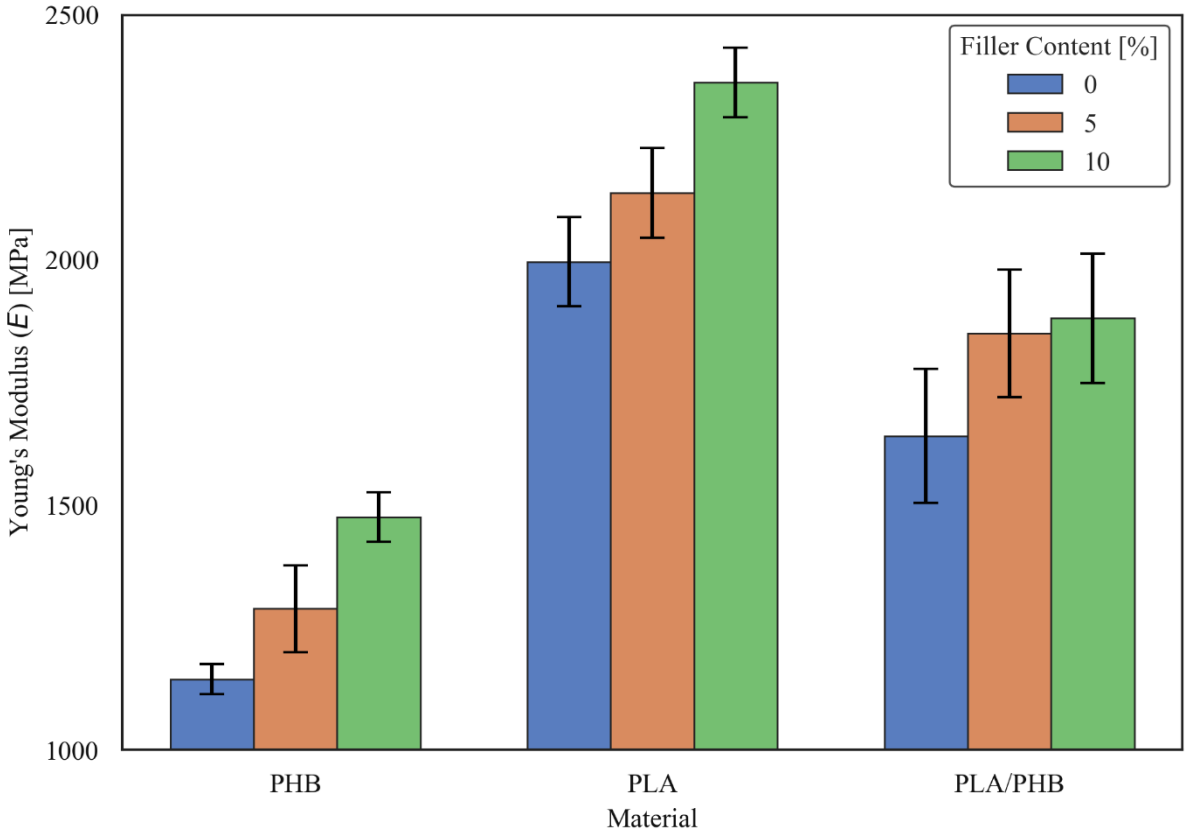

Fig. 10. Young's modulus of PLA, PHB and PLA/PHB (80:20) composites containing different amounts of wood fibers (0, 5 and 10 wt%)

The results of Young's modulus measurements indicate a clear reinforcing effect of wood fibers in all tested materials. Among the neat polymers, PLA exhibited the highest stiffness, followed by PLA/PHB (80:20) and PHB, consistent with the intrinsic stiffness of the matrices and the catalog range for PHB. In all cases, the addition of wood fibers led to an increase in Young's modulus, confirming the reinforcing effect of rigid lignocellulosic fillers. The most pronounced improvement was observed for PHB, where the modulus increased to 1475 MPa at 10 wt% filler, corresponding to an overall increase of about 29%. A similar but less pronounced trend was observed for PLA and for the PLA/PHB blend. Despite the improvement, the blend consistently showed lower stiffness than neat PLA, reflecting the softening influence of the PHB phase. Overall, these results confirm that wood fibers effectively enhance the stiffness of all studied polymer matrices, although the final modulus remains strongly dependent on the base polymer composition.

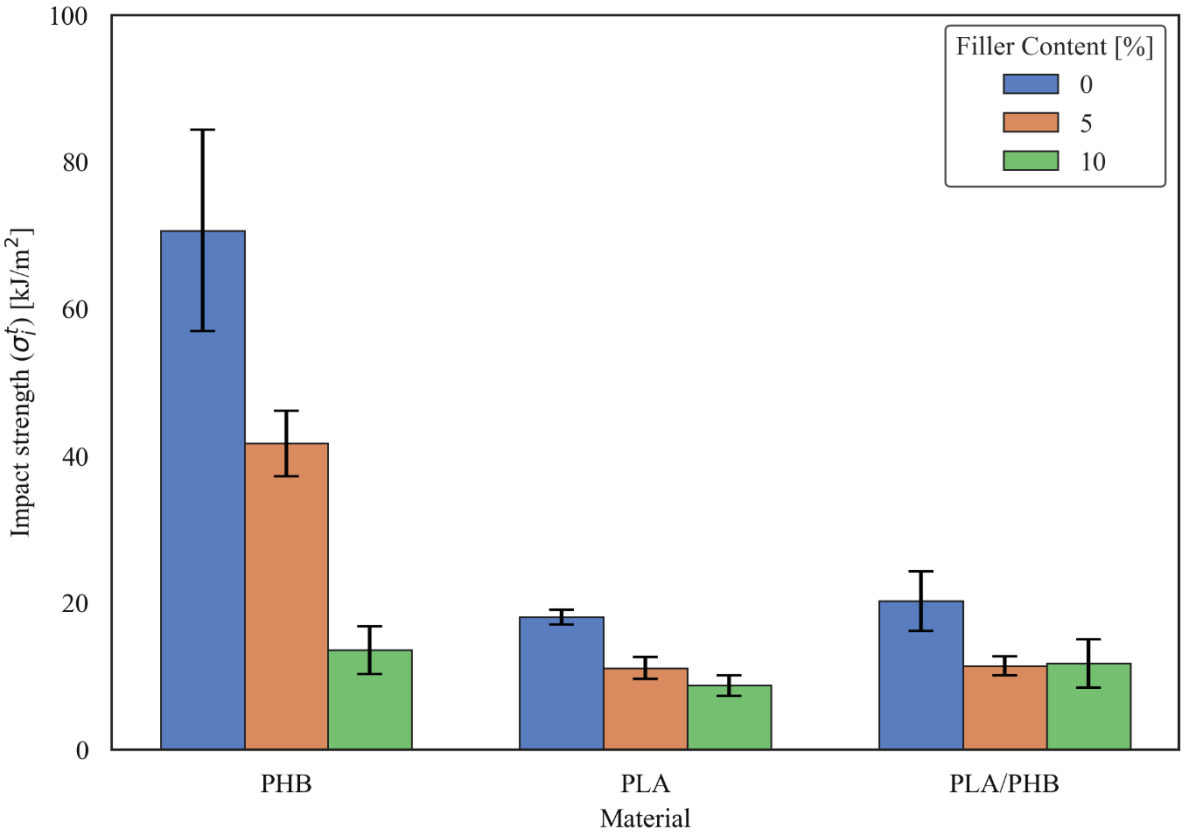

Fig. 11. Impact strength of PLA, PHB and PLA/PHB (80:20) composites containing different amounts of wood fibers (0, 5 and 10 wt%)

The impact strength results revealed a substantial decrease in toughness with increasing wood fiber content for all tested materials. Among the neat polymers, PHB exhibited the highest impact resistance (70.66 kJ/m2), which is slightly lower than the typical catalog value of approximately 82.9 kJ/m2 reported for the unnotched configuration. In all cases, wood fiber addition led to a pronounced reduction in impact strength, indicating a clear embrittlement effect. At 10 wt% filler, the impact strength decreased across all matrices. A decrease in impact strength with increasing wood fiber content in the PLA matrix has been repeatedly reported in the literature [22], which is generally attributed to stress concentration at the fiber-matrix interface. This behavior is typically associated with interfacial debonding and fiber pull-out rather than fiber fracture, which is commonly reported for lignocellulosic-reinforced PLA systems and is consistent with the observed reduction in impact resistance. The increase in impact strength observed with the addition of PHB to PLA is consistent with the findings reported in the literature [23], where Gao and Drozdov demonstrated that PLA/PHB blends exhibit a significant improvement in impact toughness, with values increasing up to approximately 40 kJ/m^2 for blends containing 40 wt% PHB. A similar trend was observed in the present study, where the incorporation of PHB led to enhanced impact performance.

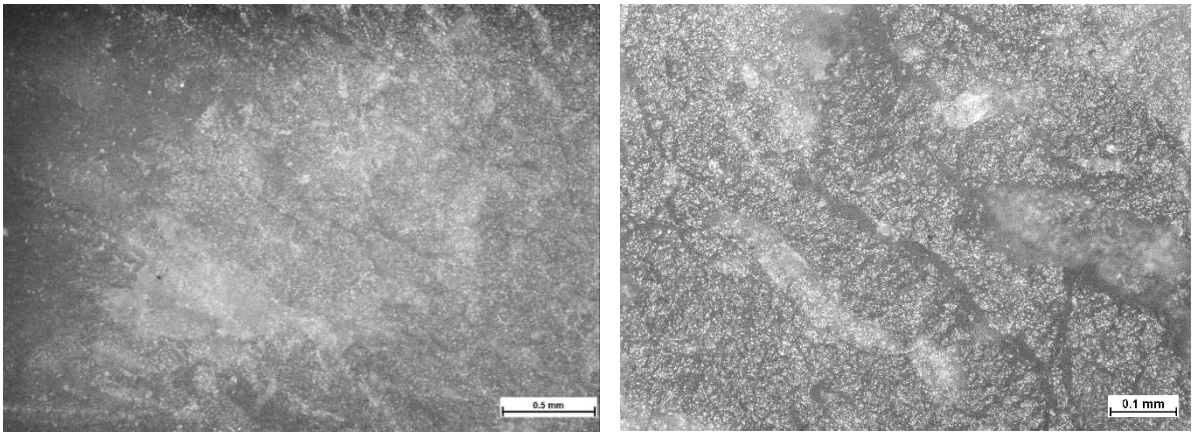

a) b)

Fig. 12. Morphology of the fracture surfaces of the PHB samples after mechanical testing: impact fracture surface at a) 2.5x and b) 10x

The surface of neat PHB is homogeneous, matte, and finely rough, without pronounced directional flow marks indicative of strong material flow (Fig. 12a). Figure 12b reveals a fine granular morphology with a network of boundaries separating individual regions. This morphology is consistent with brittle fracture in a semicrystalline polymer, where crack propagation follows weaker interfaces between crystalline domains, leading to microcrack formation rather than plastic deformation. This type of fracture, associated with the spherulitic structure and microcracking of PHB, has been reported in the literature [24].

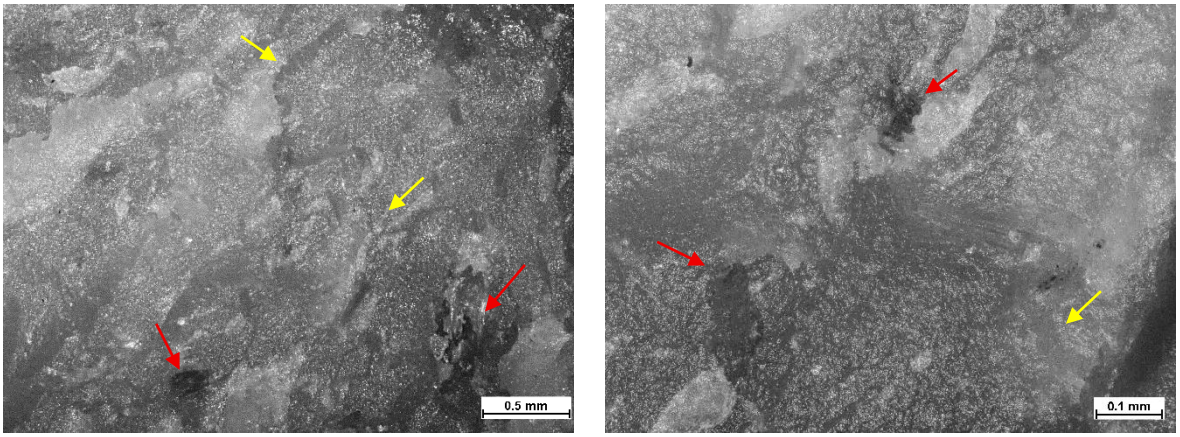

a) b)

Fig. 13. Morphology of the fracture surfaces of the PHB samples after mechanical testing containing 5 wt% of wood fibers: impact fracture surface at a) 2.5x and b) 10x. Voids are indicated by red arrows, while microcracks are marked with yellow arrows

In Figure 13a, the fracture surface of PHB samples containing 5 wt% wood fibers after mechanical testing shows a markedly more heterogeneous structure compared to neat PHB. Large areas of varying brightness and topography are visible, accompanied by localized darker regions or inclusions, which likely correspond to areas where fibers were pulled out. At the macroscopic scale brittle fracture and rapid crack propagation clearly dominate is observed. In Figure 13b, the lower regions retain the

granular texture of the matrix, similar to that seen in PHB, but additional zones with different surface features are present. The boundaries between these regions are sharper and localized discontinuities, such as dark spots, small voids, or pits, are visible. These features may arise from microvoids that develop due to fiber-matrix interfacial separation, or from microcracks initiated around dispersed particles. Similar darkened regions associated with fiber pull out and interfacial separation have also been reported in PHB composites containing organic fillers, where inadequate fiber-matrix bonding and fiber degradation during processing were shown to promote localized microvoid formation and weaken the mechanical response [25].

Voids appear as dark, irregularly shaped cavities within the material, typically corresponding to regions of trapped air or incomplete consolidation. Microcracks are observed as elongated, dark, linear features associated with damage development and propagation along weakened fiber-matrix interfaces. For clarity of interpretation, both Figures 13a and 13b are annotated to illustrate these features, where voids are marked with red arrows and microcracks with yellow arrows to support their identification across the images.

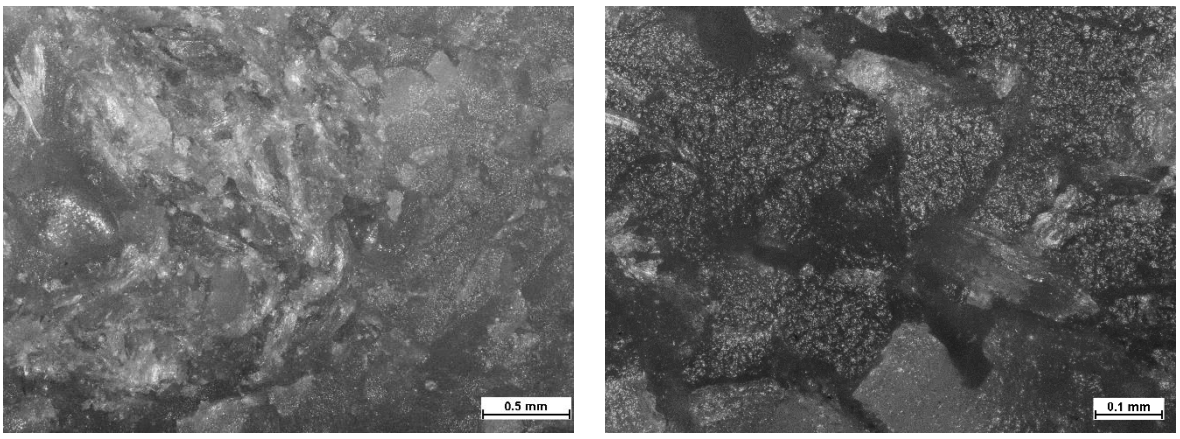

a) b)

Fig. 14. Morphology of the fracture surfaces of the PHB samples after mechanical testing containing 10 wt% of wood fibers: impact fracture surface at a) 2.5x and b) 10x

In Figure 14a, the fracture surface of PHB containing 10 wt% wood fibers shows a further increase in heterogeneity compared to the 5 wt% composite, indicating a more pronounced influence of the filler on fracture behavior. The morphology confirms dominant brittle fracture with no evidence of macroscopic plastic deformation. In Figure 14b, the granular structure of the PHB matrix is partially preserved, however, numerous discontinuities such as voids and crack-like features are present. These are attributed to coalescence of microvoids and intensified fiber-matrix debonding and pull-out. Compared to the 5 wt% composite, these effects are more extensive, reflecting increased interfacial damage at higher filler loading.

In Figure 15a, the fracture surface of PLA shows a preferential crack propagation direction with ridge-like features, indicating unstable and rapid crack growth. The morphology is characteristic of brittle fracture, with no evidence of plastic deformation or shear lip formation. At higher magnification (Figure 15b), the surface reveals step-like facets and sharp discontinuities, consistent with crack branching and coalescence during propagation. Overall, the fracture behavior confirms a brittle failure mode of PLA, in agreement with literature reports [26].

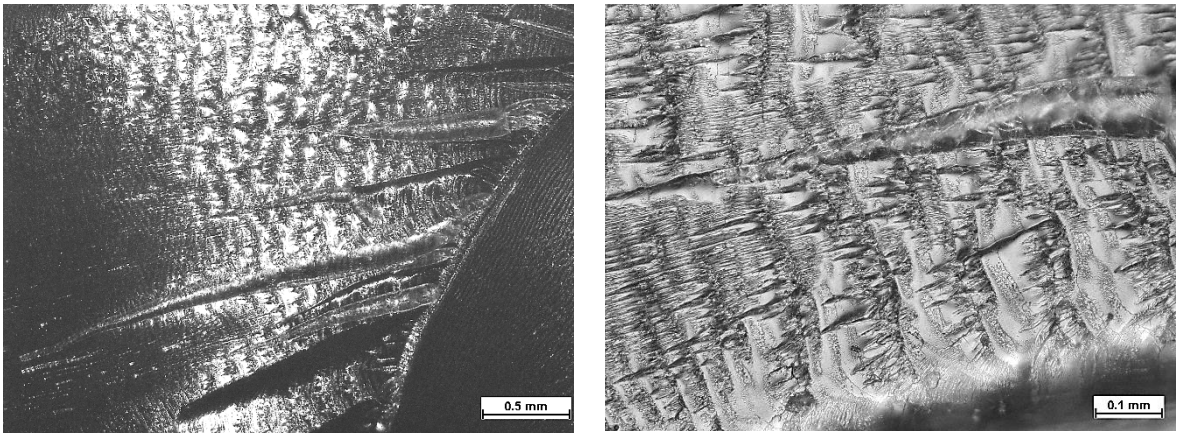

a) b)

Fig. 15. Morphology of the fracture surfaces of the PLA samples after mechanical testing: impact fracture surface at a) 2.5x and b) 10x

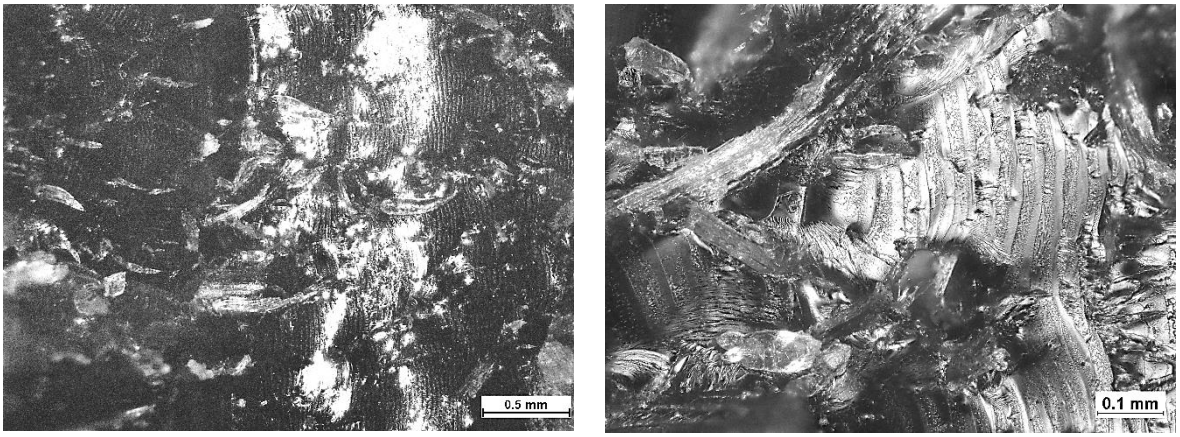

a) b)

Fig. 16. Morphology of the fracture surfaces of the PLA samples after mechanical testing containing 5 wt% of wood fibers: impact fracture surface at a) 2.5x and b) 10x

In Figure 16a, the fracture surface of PLA containing 5 wt% wood fibers shows increased heterogeneity compared to neat PLA, indicating a transition toward a more complex fracture mechanism. The morphology suggests a mixed brittle-interfacial failure mode. In Figure 16b, the presence of facets and ridges indicates localized shear deformation and matrix tearing. The crack path is deflected by the presence of fibers, promoting interfacial debonding and fiber pull-out. Overall, the addition of 5 wt% fibers modifies the fracture behavior of PLA by increasing crack path tortuosity and introducing interfacial failure mechanisms.

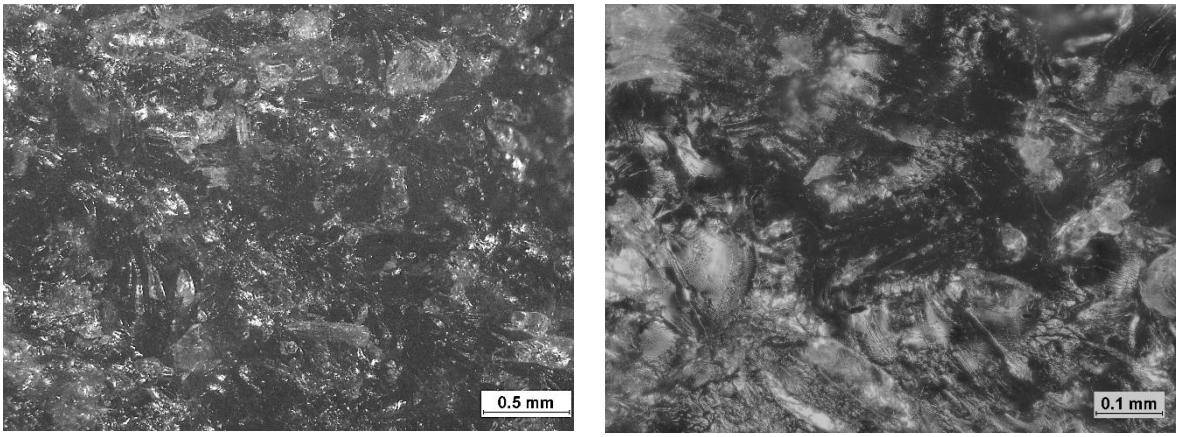

a) b)

Fig. 17. Morphology of the fracture surfaces of the PLA samples after mechanical testing containing 10 wt% of wood fibers: impact fracture surface at a) 2.5x and b) 10x

In Figure 17a, the fracture surface of PLA containing 10 wt% wood fibers shows a highly heterogeneous morphology with no preferential crack propagation direction. In Figure 17b, the presence of fragmented facets and irregular features suggests intensified matrix tearing and crack branching. Local discontinuities are associated with fiber-matrix debonding and fiber pull-out, as well as possible fiber agglomeration, which promote non-uniform stress distribution and unstable crack propagation. Compared to the 5 wt% composite, the fracture surface exhibits increased irregularity and a higher density of interfacial defects. This type of brittle fracture with evidence of fiber pull-out has also been reported for wood-fiber-reinforced PLA systems in the literature [22].

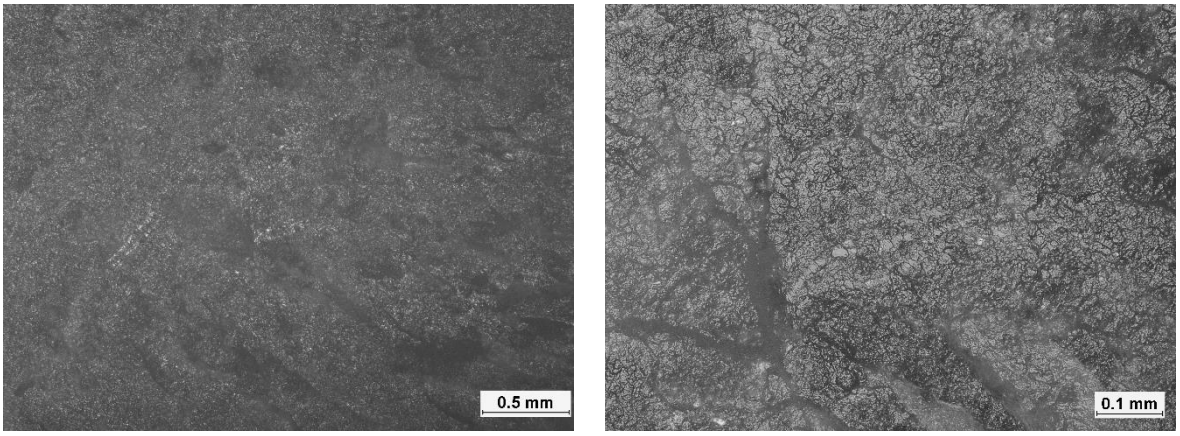

a) b)

Fig. 18. Morphology of the fracture surfaces of the PLA/PHB (80:20) samples after mechanical testing: impact fracture surface at a) 2.5x and b) 10x

In Figure 18a, the fracture surface of the PLA/PHB (80:20) blend shows a relatively homogeneous morphology without pronounced directional features, indicating a more isotropic fracture behavior compared to neat PLA. At higher magnification (Figure 18b), a fine granular network is observed, corresponding to a multiphase microstructure with dispersed PHB domains within the PLA matrix. This morphology suggests that fracture is governed primarily by the heterogeneous phase structure rather

than plastic deformation, leading to brittle crack propagation controlled by microstructural features. Similar fracture behavior in PLA/PHB (70:30) systems has been reported in the literature, where phase distribution plays a key role in crack propagation and promotes microstructure-controlled brittle failure, despite differences in blend composition [27].

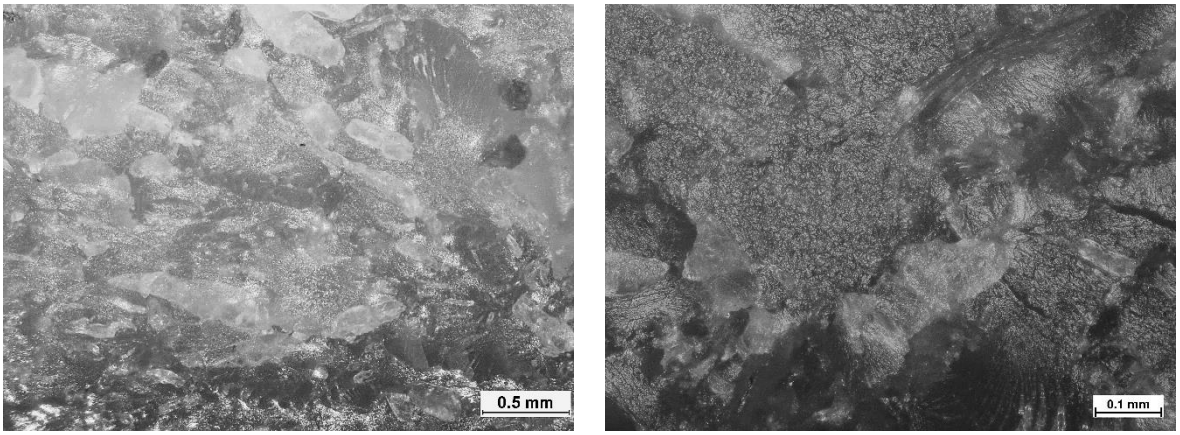

a) b)

Fig. 19. Morphology of the fracture surfaces of the PLA/PHB (80:20) samples after mechanical testing containing 5 wt% of wood fibers: impact fracture surface at a) 2.5x and b) 10x

In the PLA/PHB (80:20) blend containing 5 wt% wood fibers at lower magnification (Figure 19a) the surface is highly heterogeneous creating a complex pattern of local facets and steps. Some zones correspond to fiber pull-out, while others are associated with inclusions or agglomerates. Compared to the neat PLA/PHB (80:20) blend, the macroscale roughness is noticeably higher and the fine, uniform texture is lost. In Figure 19b, a fine granular structure similar to that seen in the neat blend is partially preserved, but is interrupted by discontinuities and voids along the boundaries of these regions. This morphology corresponds to a combination of localized fiber-matrix interfacial damage. No long, regular flow lines are present as in neat PLA.

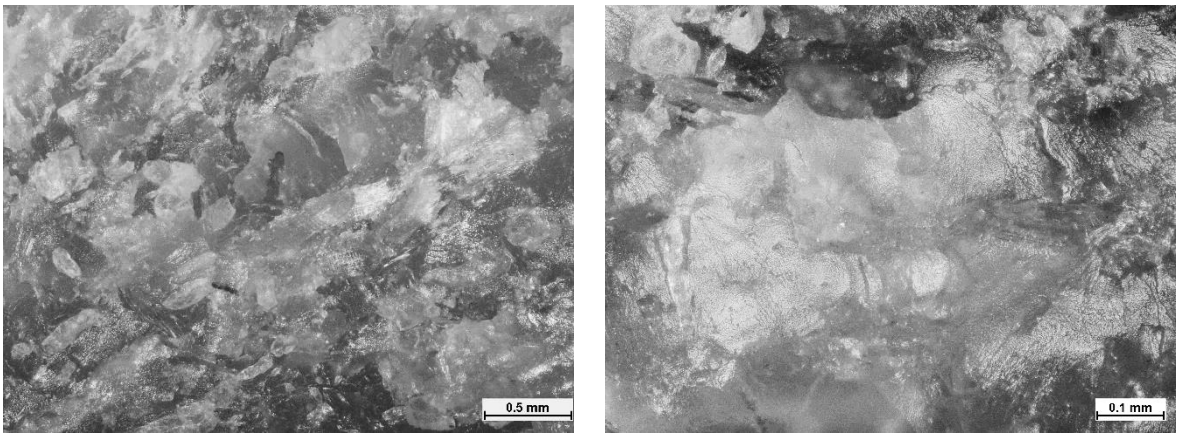

a) b)

Fig. 20. Morphology of the fracture surfaces of the PLA/PHB (80:20) samples after mechanical testing containing 10 wt% of wood fibers: impact fracture surface at a) 2.5x and b) 10x

In the PLA/PHB (80:20) blend containing 10 wt% wood fibers, cracks propagate along fiber-matrix interfaces and through local agglomerates, following paths of reduced resistance. In Figure 20a the fracture is highly heterogeneous. In Figure 20b, the surface shows reduced granular character compared to lower fiber contents, indicating a shift toward fracture dominated by weak interfacial regions. The absence of granular islands seen in lower fiber fractions indicates that the crack path is governed primarily by the weakest points e.g. fiber-matrix interfaces.

4. CONCLUSIONS

The study aimed to evaluate how the addition of wood fibers (0, 5 and 10 wt%) affects the mechanical, physical and fracture properties of injection-molded biodegradable composites based on PLA, PHB and their 80:20 blend, focusing on the resulting balance between stiffness and toughness in sustainable polymer materials, as well as the potential for reducing material costs through the incorporation of a wood-based filler while maintaining good compositional homogeneity.

PLA exhibited the highest hardness, PHB the lowest, whereas the PLA/PHB blend showed intermediate values between both neat polymers. The hardness was primarily governed by the matrix composition rather than the filler content. Increased filler loading resulted in higher variability, suggesting reduced homogeneity of the composite structure.

Density increased slightly with the addition of wood fibers for all matrices. PLA was the densest, PHB the least dense and the PLA/PHB blend showed intermediate values, with minor variability at higher filler contents.

The addition of wood fibers led to a systematic decrease in tensile strength for all material systems. PLA showed the highest tensile strength, while PHB exhibited the lowest. The PLA/PHB (80:20) blend had intermediate strength values, around 20% lower than neat PLA. Increasing filler content to 10 wt% caused a strength reduction of approximately 15-20%, depending on the matrix. The elongation at break decreased systematically with increasing filler content for all materials. PHB exhibited the highest ductility, while PLA showed the lowest. The PLA/PHB blend demonstrated intermediate elongation values, slightly higher than those of neat PLA. The addition of wood fibers caused a notable increase in Young's modulus for all polymer matrices. PLA composites exhibited the highest stiffness, followed by the PLA/PHB blend and PHB.

The incorporation of wood fibers significantly decreased impact strength for all material systems. PHB exhibited the highest impact resistance, while PLA showed the lowest. The PLA/PHB blend displayed intermediate values, closer to PLA than PHB after fiber addition. Increasing filler content from 0 to 10 wt% resulted in up to an 80% reduction in impact strength, confirming the brittle character of the composites.

The fracture surfaces were predominantly brittle and the wood fibers were generally well dispersed throughout the polymer matrices. Increasing the content of wood fibers in PHB, PLA and PLA/PHB blends results in a markedly more heterogeneous fracture surface, with visible fiber pull-out, microvoids and local defects. The addition of fibers changes the fracture mechanism from fine, quasi-brittle matrix controlled cracking to a more stepped and irregular pattern governed by fiber-matrix interfacial weaknesses. This effect becomes more pronounced at higher fiber contents, where fiber pull-out and interfacial debonding dominate over the intrinsic microstructure of the blend. The observed fracture surface features are consistent with literature reports on PHB and PLA composites with organic fillers, confirming the critical role of fiber-matrix adhesion in controlling fracture behavior.

The study demonstrates that matrix composition is the primary determinant of mechanical properties, while wood fiber addition modifies specific parameters: increasing stiffness, slightly increasing density and hardness, but reducing tensile strength, elongation, and impact resistance. The

PLA/PHB (80:20) blend exhibits intermediate behavior between neat PLA and PHB, suggesting that PHB softens the blend and enhances impact performance compared to PLA. Fiber addition introduces heterogeneity, particularly at higher contents, which governs fracture behavior and reduces ductility and toughness. These findings highlight the trade-off between reinforcement and embrittlement when incorporating natural fibers into biodegradable polymer matrices. This balance is critical for potential applications, where increased stiffness may be advantageous for packaging materials, while reduced toughness may limit suitability for load-bearing structural applications.

REFERENCES

1. Abedsoltan, H 2023. Applications of plastics in the automotive industry: Current trends and future perspectives. *Polymer Engineering & Science* **64**, 929-950.
2. Hassan, T, Saeed, S, Ahmad, A, Ahmed, F, Ali, Y and Khalid, S 2022. Synthetic polymers and their use in clinical medicine: a narrative review. *Gomal Journal of Medical Sciences* **20**, 159-164.
3. Kurowiak, J, Klekiel, T and Będziński, R 2023. Biodegradable Polymers in Biomedical Applications: A Review—Developments, Perspectives and Future Challenges. *International Journal of Molecular Sciences* **24**, 16952.
4. Cai, Z, Li, M, Zhu, Z, Wang, X, Huang, Y, Li, T, Gong, H and Yan, M 2023. Biological Degradation of Plastics and Microplastics: A Recent Perspective on Associated Mechanisms and Influencing Factors. *Microorganisms* **11**, 1661.
5. de Souza, AS, Ferreira, PG, de Jesus, IS, de Oliveira, RP, de Carvalho, AS, Futuro, DO and Ferreira, VF 2025. Recent Progress in Polyolefin Plastic: Polyethylene and Polypropylene Transformation and Depolymerization Techniques. *Molecules* **30**, 87.
6. Senila, L, Kovacs, E and Senila, M 2025. A Review of Polylactic Acid (PLA) and Poly(3-hydroxybutyrate) (PHB) as Bio-Sourced Polymers for Membrane Production Applications. *Membranes* **15**, 210.
7. Boey, JY, Mohamad, L, Khok, YS, Tay, GS and Baidurah, S 2021. A Review of the Applications and Biodegradation of Polyhydroxyalkanoates and Poly(lactic acid) and Its Composites. *Polymers* **13**, 1544.
8. Zhao, X, Hu, H, Wang, X, Yu, X, Zhou, W and Peng, S 2020. Super tough poly(lactic acid) blends: a comprehensive review. *Royal Society of Chemistry Advances* **10**, 13316-13368.
9. Meereboer, KW, Misra, M and Mohanty, AK 2020. Review of recent advances in the biodegradability of polyhydroxyalkanoate (PHA) bioplastics and their composites. *Green Chemistry* 22, 5519-5558.
10. Olejnik, O, Masek, A and Zawadziłło, J 2021. Processability and Mechanical Properties of Thermoplastic Polylactide/Polyhydroxybutyrate (PLA/PHB) Bioblends. *Materials* **14**, 898.
11. Mitaľová, Z, Mitaľ, D and Berladir, K 2024. A Concise Review of the Components and Properties of Wood-Plastic Composites. *Polymers* **16**, 1556.
12. Suriani, MJ, Ilyas, RA, Zuhri, MYM, Khalina, A, Sultan, MTH, Sapuan, SM, Ruzaidi, CM, Wan, FN, Zulkifli, F, Harussani, MM, Azman, MA, Radzi, FSM and Sharma, S 2021. Critical Review of Natural Fiber Reinforced Hybrid Composites: Processing, Properties, Applications and Cost. *Polymers* **13**, 3514.
13. Pereira, JF, Núñez, E, Reyes, A, Mali, S, Lopez-Rubio, A and Fabra, MJ 2024. On the use of lignocellulosic hemp fibers to produce biodegradable cost-efficient biocomposites. *Future Foods* **10**, 100507.

14. Łączny, D, Macko, M, Moraczewski, K, Szczepański, Z and Trafarski, A 2021. Influence of the Size of the Fiber Filler of Corn Stalks in the Polylactide Matrix Composite on the Mechanical and Thermomechanical Properties. *Materials* **14**, 7281.
15. Mulenga, T, Ude, AU and Vivekanandhan, C 2020. Concise review on the mechanical characteristics of hybrid natural fibres with filler content. *AIMS Materials Science* **7**, 650-664.
16. McKay, I, Vargas, J, Yang, L and Felfel, RM 2024. A Review of Natural Fibres and Biopolymer Composites: Progress, Limitations, and Enhancement Strategies. *Materials* **17**, 4878.
17. PN-EN ISO 527-2:2012, Plastics - Determination of tensile properties - Part 2: Test conditions for moulding and extrusion plastics.
18. PN-EN ISO 868:2005, Plastics and ebonite - Determination of indentation hardness by means of a durometer (Shore hardness).
19. PN-EN ISO 527-1:2020-01, Plastics - Determination of tensile properties - Part 1: General principles.
20. PN-EN ISO 8256:2006, Plastics - Determination of tensile-impact strength.
21. Rbihi, Z, Erchiqui, F, Rodrigue, D and Kaddami, H 2025. Thermal, Mechanical and Rheological Properties of PLA/PHB Biocomposites Reinforced with Alkaline-Treated Hemp Fibers and Granules. *ChemEngineering* **9**, 122.
22. Cosse, RL, Voet, VSD, Folkersma, R and Loos, K 2023. The effect of size and delignification on the mechanical properties of polylactic acid (PLA) biocomposites reinforced with wood fibres via extrusion. *RSC Sustainability* **1**, 876-885.
23. Gao, L and Drozdov, A 2024. Exploring the performance of bio-based PLA/PHB blends: A comprehensive analysis. *Polymers from Renewable Resources* **15**, 358-374.
24. Woo, EM and Lugito, G 2016. Cracks in Polymer Spherulites: Phenomenological Mechanisms in Correlation with Ring Bands. *Polymers* **8**, 329.
25. Vu, DH, Mahboubi, A, Ferreira, JA, Taherzadeh, MJ and Åkesson, D 2022. Polyhydroxybutyrate-Natural Fiber Reinforcement Biocomposite Production and Their Biological Recyclability through Anaerobic Digestion. *Energies* **15**, 8934.
26. Gao, H and Qiang, T 2017. Fracture Surface Morphology and Impact Strength of Cellulose/PLA Composites. *Materials* **10**, 624.
27. D'Anna, A, Arrigo, R and Frache, A 2019. PLA/PHB Blends: Biocompatibilizer Effects. *Polymers* **11**, 1416.